



Published in final edited form as:

Pancreas. 2016 March ; 45(3): 458–465. doi:10.1097/MPA.0000000000000497.

Robust Early Inflammation of the Peri-pancreatic Visceral Adipose Tissue During Diet-Induced Obesity in the KrasG12D Model of Pancreatic Cancer

Kathleen M. Hertzler, M.D., Ph.D.¹, Mu Xu, M.D., Ph.D.¹, Aune Moro, M.Sc.¹, David W. Dawson, M.D., Ph.D.², Lin Du, M.S.³, Gang Li, Ph.D.³, Hui-Hua Chang, Ph.D.¹, Alexander P. Stark, M.D.¹, Xiaoman Jung, M.D.¹, O. Joe Hines, M.D.¹, and Guido Eibl, M.D.¹

¹Department of Surgery, Laboratory Medicine, David Geffen School of Medicine at UCLA

²Department of Pathology and Laboratory Medicine, David Geffen School of Medicine at UCLA

³Department of Biostatistics, Fielding School of Public Health at UCLA, Los Angeles, CA

Abstract

Objectives—Obesity increases the incidence of multiple types of cancer. Our previous work has shown that a high fat, high calorie diet (HFCD) leads to visceral obesity, pancreatic inflammation, and accelerated pancreatic neoplasia in KrasG12D (KC) mice. In this study we aimed to investigate the effects of a HFCD on visceral adipose inflammation with emphasis on potential differences between distinct visceral adipose depots.

Methods—We examined the weight and visceral obesity in both wild-type (WT) and KC mice on either control diet (CD) or HFCD. After three months, mice were sacrificed for histological examination. Multiplex assays were also performed to obtain cytokine profiles between different adipose depots.

Results—Both WT and KC mice on a HFCD exhibited significantly increased inflammation in the visceral adipose tissue (VAT), particularly in the peri-pancreatic fat (PPF), compared to animals on a CD. This was associated with significantly increased inflammation in the pancreas. Cytokine profiles were different between visceral adipose depots, and between mice on the HFCD and CD.

Conclusions—Our results clearly demonstrate that a HFCD leads to obesity and inflammation in the VAT, particularly the PPF. These data suggest that obesity-associated inflammation in PPF may accelerate pancreatic neoplasia in KC mouse.

Keywords

Obesity; Peri-Pancreatic Fat; High Fat High Calorie Diet; Pancreatic Cancer; KrasG12D Mouse Model

Corresponding author: Guido Eibl, M.D., Department of Surgery, David Geffen School of Medicine, University of California, Los Angeles, 10833 Le Conte Avenue, 72-236 CHS, Los Angeles, CA 90095. Phone 310-825-5743; Fax: 310-825-8975; Geibl@mednet.ucla.edu.

Disclosure: The authors declare no conflict of interest.

Introduction

Pancreatic cancer (PaCa) continues to be one of the most difficult diseases to treat and it is now predicted that by 2030 it will be the second most common cause of cancer related deaths after lung cancer¹. Although very active research continues into new treatment modalities and modes of early detection, improvements in prevention and risk modification are equally or perhaps more important for altering the course of this deadly disease. One such risk factor, obesity, is the subject of much scientific investigation because it has long been acknowledged as a contributor to several major chronic health issues, including diabetes, heart disease, in addition to multiple cancer types².

Besides general obesity, excess visceral adipose tissue (VAT) has been specifically linked to an increased risk of metabolic disorders and a variety of cancers, including esophageal, colorectal, liver, and pancreatic cancers³⁻⁷. Several epidemiological studies have found the positive correlation between excessive VAT (measured by waist circumference or by CT/MRI imaging) and esophageal and colorectal cancers to be independent of BMI⁶. Excessive VAT also increases the incidence of cancer precursor lesions. For example, it is positively correlated to gastroesophageal reflux disease (GERD) and Barrett's esophagus, as well as esophageal adenocarcinoma^{8,9}. Excessive VAT also increases the incidence of non-alcoholic steatohepatitis (NASH), an increasing cause of hepatocellular carcinoma^{10,11}.

During obesity, structural and functional changes in the VAT lead to an infiltration of inflammatory cells and to different cytokine/chemokine and adipokine secretion by the adipose tissue^{12,13}. Macrophages are recruited into the VAT during obesity either as a consequence of secreted adipokines and proinflammatory cytokines or as a result from obesity-associated adipocyte necrosis. It has been shown in patients and mouse models that obesity is associated with the formation of inflammatory structures known as crown like structures (CLS) in the VAT as well as the mammary gland^{14,15}. These structures are comprised of macrophages surrounding necrotic adipocytes and are associated with increased expression of inflammatory mediators. Taken together, prevailing evidence strongly suggests that the chronic inflammatory state associated with excessive VAT facilitates oncogenic transformation and/or progression of cancer in adjacent or even distant organs. Recent studies of hormone receptor positive breast cancer in obese, post-menopausal women have linked obesity, inflammation and increased aromatase activity in breast cancer patients¹⁴. In another study, peri-prostatic adipose tissue in prostate cancer has recently been shown to influence tumor growth by promoting angiogenesis¹⁶. In addition, there is evidence that different adipose tissue depots have distinct gene expression profiles and metabolic phenotypes¹³. For example, the expression levels of TNF- α are higher in the mesenteric adipose tissue than in the omental and subcutaneous tissues, whereas leptin has a higher concentration in the subcutaneous adipose tissue than in omentum¹⁷⁻¹⁹. However, it is currently unknown whether diet-induced VAT inflammation promotes pancreatic cancer neoplasia and whether there are distinct and important differences between various visceral adipose depots.

In our previous studies we have demonstrated that a high fat, high calorie diet led to significant weight gain, metabolic disturbances, inflammation in the pancreas, and

acceleration of pancreatic neoplasia in the conditional Kras^{G12D} mouse model of pancreatic cancer²⁰. In the current work, we provide evidence that in this mouse model obesity contributes to robust VAT inflammation, in particular in the peri-pancreatic fat, which may in turn be responsible for accelerating inflammation and neoplastic progression in the adjacent pancreas.

Materials and Methods

Mouse model

The conditional Kras^{G12D} (KC) model of pancreatic cancer model from Hingorani et al. was used for this study²¹. Offspring of crosses of LSL-Kras^{G12D} and PDX-1-Cre (or p48-Cre) mice were randomly allocated to either a control diet (CD) or a high fat, high calorie diet (HFCD) for 10 weeks. Individually tagged mice had free access to the diet as well as water. Food intake and body weight of each animal were measured twice weekly. Animal studies were approved by the Chancellor's Animal Research Committee of the University of California, Los Angeles in accordance with the NIH Guide for the Care and Use of Laboratory Animals.

Genotyping analysis

Prior to randomization to the study diets, the presence of the of the Kras^{G12D} and Cre allele were determined by PCR analysis of genomic DNA, as described elsewhere²². Animals with both the Kras^{G12D} and Cre alleles were designated as mutant (KRAS^{+G12D}) and animals with neither the Kras^{G12D} nor the Cre allele were deemed wild-type (KRAS^{+/+}). At the end of the study at sacrifice the successful excision-recombination events were confirmed by PCR by the presence of a single LoxP site in the pancreas as described elsewhere²².

Experimental diets

The diets were obtained from Dyets, Inc., Pennsylvania. Weaned mice were allocated to either a CD or a HFCD as described previously²⁰. Briefly, 40% and 12% of calories were derived from fat (corn oil based) in the HFCD and CD, respectively. The diets were handled under low light conditions, and stored at -20°C. The diets were replaced twice weekly. The stability of the fatty acids in the diets was regularly monitored by the UCLA Nutritional Biomarker and Phytochemistry Core.

Sample preparation

The visceral organs (including liver and pancreas) as well as various fat depots were either snap frozen immediately after dissection in liquid nitrogen and stored at -80C until further processing, or fixed in a solution of 10% formalin and subsequently paraffin embedded. Adipose tissue near the gonads was designated as visceral fat (VF) and adipose tissue adjacent and overlaying the pancreas was labeled peri-pancreatic fat (PPF).

Quantification of adipose tissue volume

Prior to sacrifice, all mice were imaged by micro-CT at the UCLA Pre-Clinical Imaging Center. Total VAT was quantified as a fraction of the total abdominal soft tissue volume

based on Hounsfield units in a selected area of the upper abdomen. Adipose tissue was defined as tissue within the range of -270 to -100 Hounsfield units, whereas -270 to 500 Hounsfield units were used for total soft tissue.

Adipose tissue histology

Tissues were fixed in phosphate buffered formalin for 24 hours and subsequently embedded in paraffin. Sections ($4\ \mu\text{m}$ thick) were mounted onto slides and stained with H&E. Slides were imaged on a Nikon Eclipse 90i microscope and bright field images were acquired with NIS AR4.2 software (Nikon). Adipose tissue sections were examined for evidence of inflammatory infiltrates or for determination of adipocyte size. Inflammatory foci were quantified using a $10\times$ objective and described as number per HPF. An inflammatory focus was defined as one adipocyte at least partially surrounded by inflammatory cells (crown like structures; CLS) and larger lymphoid aggregates. Ten images were taken per mouse and the number of inflammatory foci and the area of ten randomly chosen adipocytes per HPF were measured.

Cytokine assays

Snap frozen mouse adipose tissue (VF or PPF) was defrosted on ice and homogenized with a mechanical homogenizer in $1\times\text{PBS}$, pH 7.2, $1\ \text{mmol/L}$ phenylmethylsulfonylfluoride (Sigma-Aldrich) with protease inhibitors (Complete Protease Inhibitor Cocktail Tablet, Roche) and subsequently sonicated. Lysates were then centrifuged at 4°C for 15 minutes at $14,000\ \text{rpm}$ and the supernatant was separated from the pellet using a 26 gauge needle and syringe. Protein concentrations were determined by bicinchoninic acid protein assay (Thermo Scientific) with bovine serum albumin as a standard. Lysates were diluted to $1\ \text{mg/ml}$ total protein concentration and applied to a mouse cytokine magnetic bead panel (EMD Millipore) in a 96-well plate format. Duplicates of each sample were incubated overnight on a rotary orbital shaker at 4°C . Plates were then processed as recommended by the manufacturer and samples were run using a Bio-Plex 200 HTF Analyzer Luminex system (Bio-Rad). Data were obtained with Bio-Plex Manager 6.1 software (Bio-Rad) and further analyzed with Microsoft Excel.

Pancreas histology

Sections of the pancreas of each animal were stained with hematoxylin and eosin (H&E) and analyzed by a GI pathologist (D. Dawson) blinded to treatment conditions. Inflammation was graded as previously described (Dawson 2013). Briefly, acinar loss was based on the percentage loss across the entire cross-section and graded as 0=absent; 1=1–25%; 2=26–50%; 3=51–75%; 4>75%. Inflammation was based on the average number of lobular inflammatory cells per $40\times$ high-power field (HPF; as counted in 10 non-overlapping HPFs) and graded as 0=absent; 1=1–30 cells; 2=31–50 cells; 3=51–100 cells; 4>100 cells. Fibrosis was based on the cumulative area of stromal fibrosis across the entire pancreas and graded as 0=absent; 1=1–5%; 2=6–10%; 3=11–20%; 4=>20%. Murine PanINs were classified according to histopathologic criteria as previously described²⁰. The total number of ductal lesions and their grade were determined. Only the highest grade lesion per pancreatic lobule was evaluated. About 100 pancreatic ducts of the entire fixed specimen (head, body, and tail

of the pancreas) were analyzed for each animal. The relative proportion of each mPanIN to the overall number of analyzed ducts was recorded for each animal.

Statistical analysis

Values are presented as mean \pm SEM. Significance was determined using an unpaired t test, with significance determined at a p-value of <0.05 . To analyze the number of lymphoid aggregates, 2×2 contingency tables were constructed and a chi-square test for contingency was used. A one-sided Fisher's exact test was then applied to each individual cohort to determine significance.

Results

A HFCD increases total visceral fat volume in WT and KC mice

Both WT and KC mice were fed the CD or HFCD for a total of 10 weeks. WT male and female mice gained approximately 2-fold more weight on a HFCD than on a CD, while KC mice gained ~ 1.4 fold more weight on a HFCD (Figure 1). In order to determine how the overall weight gain correlated to the expansion of the VAT, all mice were imaged by micro-CT prior to sacrifice. Using a defined area of the upper abdomen, total VAT gain was measured as a fraction of total soft tissue in the same region. WT mice on a HFCD gained approximately 2-fold more total VAT than WT mice fed a CD ($p < 0.05$) (Figure 1). The enlargement of the VAT correlated strongly with weight gain (Pearson correlation coefficient > 0.9 ; not shown). KC mice also showed an increase in the VAT volume as quantified by micro-CT. While male KC mice gained ~ 2 -fold more VAT volume than their CD counterparts (similar to WT mice) female KC mice fed the HFCD did not significantly increase their total VAT volume (Figure 1). In general, female mice gained less weight than their male counterparts and KC mice gained less weight than WT mice. However, these results demonstrate that both WT and KC mice gain weight on a HFCD and the weight gain overall correlates strongly with an enlargement of the total VAT.

Different visceral adipose depots in both WT and KC mice display distinct inflammatory responses to the HFCD

The VAT of animals on a HFCD has been shown to exhibit crown like structures (CLS), in which necrotic adipocytes are surrounded by inflammatory cells, including macrophages^{23–25}. Since there is evidence in the literature that different adipose depots in the abdomen display distinct metabolic phenotypes¹³, we examined specifically the visceral adipose depots adjacent to the pancreas (peri-pancreatic fat; PPF) and distant to the pancreas around the gonads (visceral fat; VF) for evidence of these inflammatory structures. There was very little evidence of inflammation in the VF or PPF of female and male WT mice on a CD (Figure 2A). Interestingly, while there was little inflammation in the VF of male and female KC mice on a CD, a significantly increased number of inflammatory foci was seen in the PPF of male and female KC mice fed the CD (Figure 2B). When fed the HFCD, a robust increase in inflammatory foci was observed in the VF and PPF of WT male mice (Figure 2A). While the HFCD failed to increase the presence of inflammatory foci in the VF of female WT and KC mice, a significant increase in the number of these inflammatory structures was found in the PPF (Figure 2A, B).

We noted that the inflammatory foci in the PPF often tended to be larger and in the form of lymphoid aggregates (Figure 2A, arrowhead). We then counted the number of mice, in which large lymphoid aggregates in either the VF or the PPF were seen (Figure 2C). Overall, lymphoid aggregates occurred more often in PPF than in the VF ($p < 0.0001$). Further analyses showed that lymphoid aggregates occurred more often in the PPF than in the VF in female WT mice fed the HFCD, male and female KC mice fed the HFCD (Figure 2C). In addition, lymphoid aggregates were found to occur more often in KC mice compared to WT mice and in mice fed the HFCD (compared to CD) (Figure 2C).

There is evidence in the literature that the distinct metabolic phenotypes of different visceral adipose depots often correspond to different sizes of individual adipocytes¹³. In order to evaluate whether the PPF and VF in our model exhibit potentially different metabolic phenotypes, we quantified the size (area) of individual adipocytes in both VF and PPF. For both WT and KC mice, adipocytes in the PPF are significantly smaller than those in the VF (Figures 3A, B). In addition, the HFCD significantly increased adipocyte size in both VF and PPF. However, the effect of the HFCD on adipocyte size was significantly more robust in the VF than in the PPF.

Cytokine expression varies among different visceral fat depots

Having demonstrated that the HFCD causes distinct inflammatory changes histologically in both the VF and PPF, we next investigated whether the VF and PPF showed differences in cytokine expression. We employed a multiplex cytokine assay platform to measure immunomodulatory cytokines from the VAT lysates of both WT and KC mice. In both WT and KC mice fed the CD, several cytokines showed clear differences in expression between the VF and PPF (Figures 4A, B). Most frequently, baseline expression of these cytokines was increased in the PPF compared to the VF. In addition, the HFCD increased the expression of certain cytokines specifically in the PPF but not in the VF (Figure 4C). Taken together, these data clearly indicate that functional differences, as measured by cytokine expression (baseline and in response to the diet), exist between the VF and PPF in both WT and KC mice.

A HFCD leads to pancreatic inflammation in WT and KC mice

We then examined whether the inflammatory changes in the visceral adipose tissue correlate to histologic changes in the pancreas. After 10 weeks, mice fed the HFCD showed significant inflammation in the pancreas (Figure 5A), which is exemplified by a loss of normal acinar structure ($12 \pm 4\%$ CD vs. $37 \pm 10\%$ HFCD), an increase in inflammatory cell infiltration (11 ± 4 CD vs. 26 ± 6 HFCD), and by an increase in stromal fibrosis ($5 \pm 2\%$ CD vs. $20 \pm 6\%$ HFCD). There was a trend towards slightly more PanIN1b and PanIN2 in KC mice on a HFCD (compared to CD), although these changes did not reach statistical significance at 10 weeks (Figure 5B). In WT mice, no evidence of neoplasia was seen, although evidence of pancreatic inflammation was seen in mice fed the HFCD (data not shown). These results show that feeding a HFCD for 10 weeks creates a significantly more robust inflammatory environment in the pancreas (compared to CD-fed mice); however at this early stage no significant differences in neoplastic lesions in the pancreas can be found between the CD- and HFCD-fed KC mice.

Discussion

The most salient finding of this study is the observation that in the conditional KrasG12D mouse model of pancreatic cancer a diet high in fat and calories is associated with robust inflammation in the VAT, especially in the peri-pancreatic region, which seems histologically and functionally different than the adipose tissue in other visceral regions, e.g. peri-gonadal. This notion is supported by 1) enhanced inflammation in the PPF as demonstrated histologically by an increased number of inflammatory foci; 2) smaller adipocyte size; and 3) different cytokine profile. Previous studies by other investigators have shown that different visceral adipose depots have distinct characteristics, such as adipogenesis, replication, and susceptibility to senescence^{13,26,27}.

There is very little knowledge about the role of the PPF in human pancreatic disease. In severe acute pancreatitis, PPF necrosis has been correlated with disease severity²⁸. In PaCa, invasion of the PPF by the cancer cells was identified as an independent predictor of poor outcome following pancreateoduodenectomy^{29–31}. PEDF (pigmented epithelium-derived factor) deficiency in the Ela(elastase)-Kras mouse model led to invasive PaCa that was associated with enlarged PPF³², suggesting an association between the PPF and progression of pancreatic ductal adenocarcinoma. PEDF was recently found to have an anti-obesity effect by counteracting insulin resistance and suppress pancreatic tumor growth at high concentrations³³. In contrast, PEDF null mice have truncal obesity and increased PPF³⁴.

It is unclear where anatomically the PPF originates. It is conceivable that the PPF belongs to the mesenteric adipose tissue based on their anatomical proximity. Adipose tissue derived mesenchymal stem cells have the capacity to migrate to the site with tissue injury^{35,36}. Whether the expression of an oncogenic Kras or the presence of diet-induced inflammation in the pancreas serves as a chemotactic factor in recruiting mesenchymal stem cells to the peri-pancreatic location is currently unknown. Our data also demonstrate a more robust increase in visceral adipose tissue inflammation in male mice fed the HFCD, compared to female mice. This correlated to a more enlarged visceral adipose tissue volume in HFCD-fed male mice as measured by CT. This observation that compared to female mice male mice respond stronger to the HFCD in terms of visceral adipose tissue expansion and inflammation reflects the human conditions, although the underlying potentially hormonal reasons are unclear in this model. In our study, the inflammatory changes in the VAT of HFCD-fed mice correlated with an enhanced inflammatory reaction in the pancreas, but occurred prior to significant differences in PanIN development. In a prior study we demonstrated that diet-induced obesity was associated with an accelerated pancreatic neoplasia in slightly older animals²⁰. Together, these results suggest that the formation of a diet-induced inflammatory micro-environment (in the VAT and pancreas) precedes the acceleration of pancreatic neoplasia in this model. It is currently unclear how exactly the HFCD causes pancreatic inflammation in our model. It is conceivable that the HFCD has direct effects on the pancreas causing tissue inflammation. However, it is also plausible that the HFCD initially induces adipose tissue inflammation, which leads to inflammation in neighboring organs, e.g. pancreas, through secretion of inflammatory cytokines from the visceral adipose tissue. Our observation that KC mice fed the HFCD show more robust signs

of pancreatic inflammation, compared to wildtype mice fed the HFCD, strongly suggest a cross-talk between the oncogenic Kras and the HFCD.

Our results implicate that VAT inflammation associated with obesity might be an intriguing target to prevent PaCa development. Bariatric surgery has become the standard treatment for morbidly obese patients. It can decrease the size of PPF⁴⁰. Long-term follow-up after bariatric surgery has confirmed significant weight loss as well as a decrease in the occurrence of multiple cancer types, in particular, breast and endometrial cancer^{41–43}. Medical therapy has also shown promising results. A recent study showed that thiazolidinediones (TZD), a PPAR (peroxisome proliferator-activated receptors) ligand, can decrease inflammation in the adipose tissue and reduce the size of PPF⁴⁴. Metformin, which is well known to increase insulin sensitivity and cause weight loss in obese patients, has been shown to reduce the risk of PaCa in type II diabetes, as well as many other cancers^{45,46}.

In conclusion, our results show that a HFCD leads to increased inflammation of the VAT, particularly in the peri-pancreatic region, in the KC mouse model of PaCa. The enhanced VAT inflammation was associated with increased pancreatic inflammation but occurred prior to the development of pancreatic neoplasia. Together with our previous report showing enhanced pancreatic neoplasia in KC mice fed a HFCD for a longer period of time, these results strongly suggest an important and early role of VAT inflammation in pancreatic cancer development.

Acknowledgments

Grant support:

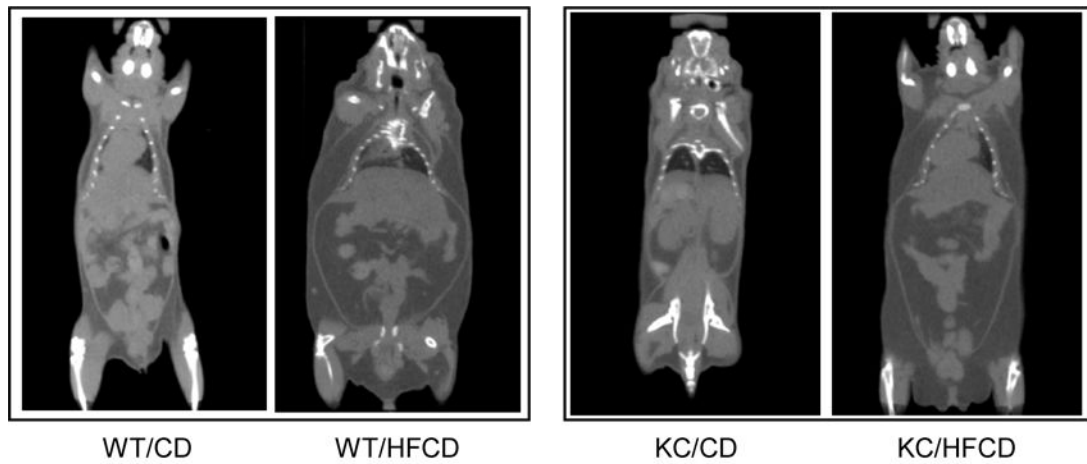
National Institutes of Health (P01CA163200, DK41301, UL1TR000124, T32 Gastroenterology Training Grant DK07180-40) and the Hirshberg Foundation for Pancreatic Cancer Research

References

1. Rahib L, Smith BD, Aizenberg R, et al. Projecting cancer incidence and deaths to 2030: the unexpected burden of thyroid, liver, and pancreas cancers in the United States. *Cancer Res.* 2014; 74:2913–2921. [PubMed: 24840647]
2. Thiebaut AC, Jiao L, Silverman DT, et al. Dietary fatty acids and pancreatic cancer in the NIH-AARP diet and health study. *J Natl Cancer Inst.* 2009; 101:1001–1011. [PubMed: 19561318]
3. Alexopoulos N, Katritsis D, Raggi P. Visceral adipose tissue as a source of inflammation and promoter of atherosclerosis. *Atherosclerosis.* 2014; 233:104–112. [PubMed: 24529130]
4. Blüner M. Adipose tissue dysfunction contributes to obesity related metabolic diseases. *Best Pract Res Clinl Endocrinol Metabolism.* 2013; 27:163–177.
5. Kredel LI, Siegmund B. Adipose-tissue and intestinal inflammation - visceral obesity and creeping fat. *Front Immunol.* 2014; 5:462. [PubMed: 25309544]
6. Vongsuvan R, George J, Qiao L, et al. Visceral adiposity in gastrointestinal and hepatic carcinogenesis. *Cancer Lett.* 2013; 330:1–10. [PubMed: 23201597]
7. Mantovani A, Allavena P, Sica A, et al. Cancer-related inflammation. *Nature.* 2008; 454:436–444. [PubMed: 18650914]
8. El-Serag HB, Kvapil P, Hacken-Bitar J, et al. Abdominal obesity and the risk of Barrett's esophagus. *Am J Gastroenterol.* 2005; 100:2151–2156. [PubMed: 16181362]

9. Steffen A, Schulze MB, Pischon T, et al. Anthropometry and esophageal cancer risk in the European prospective investigation into cancer and nutrition. *Cancer Epidemiol Biomarkers Prev.* 2009; 18(7): 2079–2089. [PubMed: 19567501]
10. Nault JC, Zucman-Rossi J. Building a bridge between obesity, inflammation and liver carcinogenesis. *J Hepatol.* 2010; 53(4):777–779. [PubMed: 20633947]
11. Schlesinger S, Aleksandrova K, Pischon T, et al. Abdominal obesity, weight gain during adulthood and risk of liver and biliary tract cancer in a European cohort. *Int J Cancer.* 2013; 132:645–657. [PubMed: 22618881]
12. Lysaght J, van der Stok EP, Allott EH, et al. Pro-inflammatory and tumour proliferative properties of excess visceral adipose tissue. *Cancer Lett.* 2011; 312:62–72. [PubMed: 21890265]
13. Tchkonja T, Thomou T, Zhu Y, et al. Mechanisms and metabolic implications of regional differences among fat depots. *Cell Metab.* 2013; 17:644–656. [PubMed: 23583168]
14. Morris PG, Hudis CA, Giri D, et al. Inflammation and increased aromatase expression occur in the breast tissue of obese women with breast cancer. *Cancer Prev Res.* 2011; 4:1021–1029.
15. Subbaramaiah K, Howe LR, Bhardwaj P, et al. Obesity is associated with inflammation and elevated aromatase expression in the mouse mammary gland. *Cancer Prev Res.* 2011; 4:329–346.
16. Venkatasubramanian PN, Brendler CB, Plunkett BA, et al. Periprostatic adipose tissue from obese prostate cancer patients promotes tumor and endothelial cell proliferation: A functional and MR imaging pilot study. *Prostate.* 2014; 74:326–335. [PubMed: 24571013]
17. Cartier A, Lemieux I, Almeras N, et al. Visceral obesity and plasma glucose-insulin homeostasis: contributions of interleukin-6 and tumor necrosis factor-alpha in men. *J Clin Endocrinol Metab.* 2008; 93:1931–1938. [PubMed: 18319319]
18. Xu XJ, Gauthier MS, Hess DT, et al. Insulin sensitive and resistant obesity in humans: AMPK activity, oxidative stress, and depot-specific changes in gene expression in adipose tissue. *J Lipid Res.* 2012; 53:792–801. [PubMed: 22323564]
19. Wiest R, Moleda L, Farkas S, et al. Splanchnic concentrations and postprandial release of visceral adipokines. *Metabolism.* 2010; 59:664–670. [PubMed: 19913846]
20. Dawson DW, H K, Moro A, Donald G, Chang HH, et al. High-fat, high-calorie diet promotes early pancreatic neoplasia in the conditional KrasG12D mouse model. *Cancer Prev Res.* 2013; 6:1064–1073.
21. Hingorani S, Petricoin EF, Maitra A, et al. Preinvasive and invasive ductal pancreatic cancer and its early detection in the mouse. *Cancer Cell.* 2003; 4:437–450. [PubMed: 14706336]
22. Funahashi H, Satake M, Dawson D, et al. Delayed progression of pancreatic intraepithelial neoplasia in a conditional Kras(G12D) mouse model by a selective cyclooxygenase-2 inhibitor. *Cancer research.* 2007; 67:7068–7071. [PubMed: 17652141]
23. Canello R, Henegar C, Viguerie N, et al. Reduction of Macrophage Infiltration and Chemoattractant Gene Expression Changes in White Adipose Tissue of Morbidly Obese Subjects After Surgery-Induced Weight Loss. *Diabetes.* 2005; 54:2277–2286. [PubMed: 16046292]
24. Cinti S, Mitchell G, Barbatelli G, et al. Adipocyte death defines macrophage localization and function in adipose tissue of obese mice and humans. *J Lipid Res.* 2005; 46:2347–2355. [PubMed: 16150820]
25. Murano I, Barbatelli G, Parisani V, et al. Dead adipocytes, detected as crown-like structures, are prevalent in visceral fat depots of genetically obese mice. *J Lipid Res.* 2008; 49:1562–1568. [PubMed: 18390487]
26. Wang H, Kirkland JL, Hollenberg CH. Varying capacities for replication of rat adipocyte precursor clones and adipose tissue growth. *J Clin Invest.* 1989; 83:1741–1746. [PubMed: 2708530]
27. Kirkland JL. Age, anatomic site, and the replication and differentiation of adipocyte precursors. *Am J Physiol.* 1990; 258:C206–210. [PubMed: 2305864]
28. Yashima Y, Isayama H, Tsujino T, et al. A large volume of visceral adipose tissue leads to severe acute pancreatitis. *J Gastroenterol.* 2011; 46:1213–1218. [PubMed: 21805069]
29. Mathur A, Zyromski NJ, Pitt HA, et al. Pancreatic steatosis promotes dissemination and lethality of pancreatic cancer. *J Am Coll Surg.* 2009; 208:989–994. discussion 994–996. [PubMed: 19476877]
30. Zyromski NJ, Mathur A, Pitt HA, et al. Obesity potentiates the growth and dissemination of pancreatic cancer. *Surgery.* 2009; 146:258–263. [PubMed: 19628082]

31. Jamieson NB, Foulis AK, Oien KA, et al. Peripancreatic fat invasion is an independent predictor of poor outcome following pancreaticoduodenectomy for pancreatic ductal adenocarcinoma. *J Gastrointest Surg.* 2011; 15:512–524. [PubMed: 21116727]
32. Grippo PJ, Fitchev PS, Bentrem DJ, et al. Concurrent PEDF deficiency and Kras mutation induce invasive pancreatic cancer and adipose-rich stroma in mice. *Gut.* 2012; 61:1454–1464. [PubMed: 22234980]
33. Yamagishi S, Matsui T, Takenaka K, et al. Pigment epithelium-derived factor (PEDF) prevents platelet activation and aggregation in diabetic rats by blocking deleterious effects of advanced glycation end products (AGEs). *Diabetes Metab Res Rev.* 2009; 25:266–271. [PubMed: 19165765]
34. Yoshida T, Yamagishi S, Nakamura K, et al. Pigment epithelium-derived factor (PEDF) ameliorates advanced glycation end product (AGE)-induced hepatic insulin resistance in vitro by suppressing Rac-1 activation. *Horm Metab Res.* 2008; 40:620–625. [PubMed: 18792873]
35. Banas A, Teratani T, Yamamoto Y, et al. Rapid hepatic fate specification of adipose-derived stem cells and their therapeutic potential for liver failure. *J Gastroenterol Hepatol.* 2009; 24:70–77. [PubMed: 18624899]
36. Cai L, Johnstone BH, Cook TG, et al. IFATS collection: Human adipose tissue-derived stem cells induce angiogenesis and nerve sprouting following myocardial infarction, in conjunction with potent preservation of cardiac function. *Stem Cells.* 2009; 27:230–237. [PubMed: 18772313]
37. Cheon EC, Strouch MJ, Barron MR, et al. Alteration of strain background and a high omega-6 fat diet induces earlier onset of pancreatic neoplasia in EL-Kras transgenic mice. *Int J Cancer.* 2011; 128:2783–2792. [PubMed: 20725998]
38. Philip B, Roland CL, Daniluk J, et al. A high-fat diet activates oncogenic Kras and COX2 to induce development of pancreatic ductal adenocarcinoma in mice. *Gastroenterology.* 2013; 145:1449–1458. [PubMed: 23958541]
39. Borrello MG, Alberti L, Fischer A, et al. Induction of a proinflammatory program in normal human thyrocytes by the RET/PTC1 oncogene. *Proc Natl Acad Sci U S A.* 2005; 102:14825–14830. [PubMed: 16203990]
40. Gaborit B, Abdesselam I, Kober F, et al. Ectopic fat storage in the pancreas using H-MRS: importance of diabetic status and modulation with bariatric surgery-induced weight loss. *Int J Obes (Lond).* 2015; 39:480–487. [PubMed: 25042860]
41. Christou NV, Lieberman M, Sampalis F, et al. Bariatric surgery reduces cancer risk in morbidly obese patients. *Surg Obes Relat Dis.* 2008; 4:691–695. [PubMed: 19026373]
42. Sjöström L, Gummesson A, Sjöström CD, et al. Effects of bariatric surgery on cancer incidence in obese patients in Sweden (Swedish Obese Subjects Study): a prospective, controlled intervention trial. *Lancet Oncol.* 2009; 10:653–662. [PubMed: 19556163]
43. McCawley GM, Ferriss JS, Geffel D, et al. Cancer in obese women: potential protective impact of bariatric surgery. *J Am Coll Surg.* 2009; 208:1093–1098. [PubMed: 19476897]
44. Jilkova ZM, Hensler M, Medrikova D, et al. Adipose tissue-related proteins locally associated with resolution of inflammation in obese mice. *Int J Obes (Lond).* 2014; 38:216–223. [PubMed: 23756677]
45. Wang Z, Lai ST, Xie L, et al. Metformin is associated with reduced risk of pancreatic cancer in patients with type 2 diabetes mellitus: a systematic review and meta-analysis. *Diabetes Res Clin Pract.* 2014; 106:19–26. [PubMed: 24837144]
46. Lee A, Morley JE. Metformin Decreases Food Consumption and Induces Weight Loss in Subjects with Obesity with Type II Non-Insulin-Dependent Diabetes. *Obes Res.* 1998; 6:47–53. [PubMed: 9526970]



WT	Net Weight Gain ± SEM (gm)	Fraction Fat ± SEM	KrasG12D	Net Weight Gain ± SEM (gm)	Fraction Fat ± SEM
M/CD	9.6 ± 0.7	0.25 ± 0.07	M/CD	9.6 ± 0.8	0.13 ± 0.04
M/HFCD	17.9 ± 0.9 *	0.50 ± 0.03 *	M/HFCD	13.0 ± 1.1 *	0.24 ± 0.05 *
F/CD	6.5 ± 0.8	0.14 ± 0.09	F/CD	6.0 ± 0.8	0.10 ± 0.03
F/HFCD	11.9 ± 0.7 *	0.27 ± 0.05 *	F/HFCD	8.1 ± 0.5 *	0.11 ± 0.04

Figure 1.

Wild-type (WT) and KrasG12D (KC) mice were allocated randomly to a CD or HFCD for 10 weeks. Net gain in grams (gm) ± standard error of the mean (SEM) was calculated at the end of the experiment. All mice were imaged by micro-CT (representative images in the upper row). Visceral adipose tissue (VAT) was quantified as a fraction of fat volume per total abdominal tissue ± SEM based on Hounsfield units in a selected area of the upper abdomen using Amide software. *, $p < 0.05$, HFCD vs. CD.

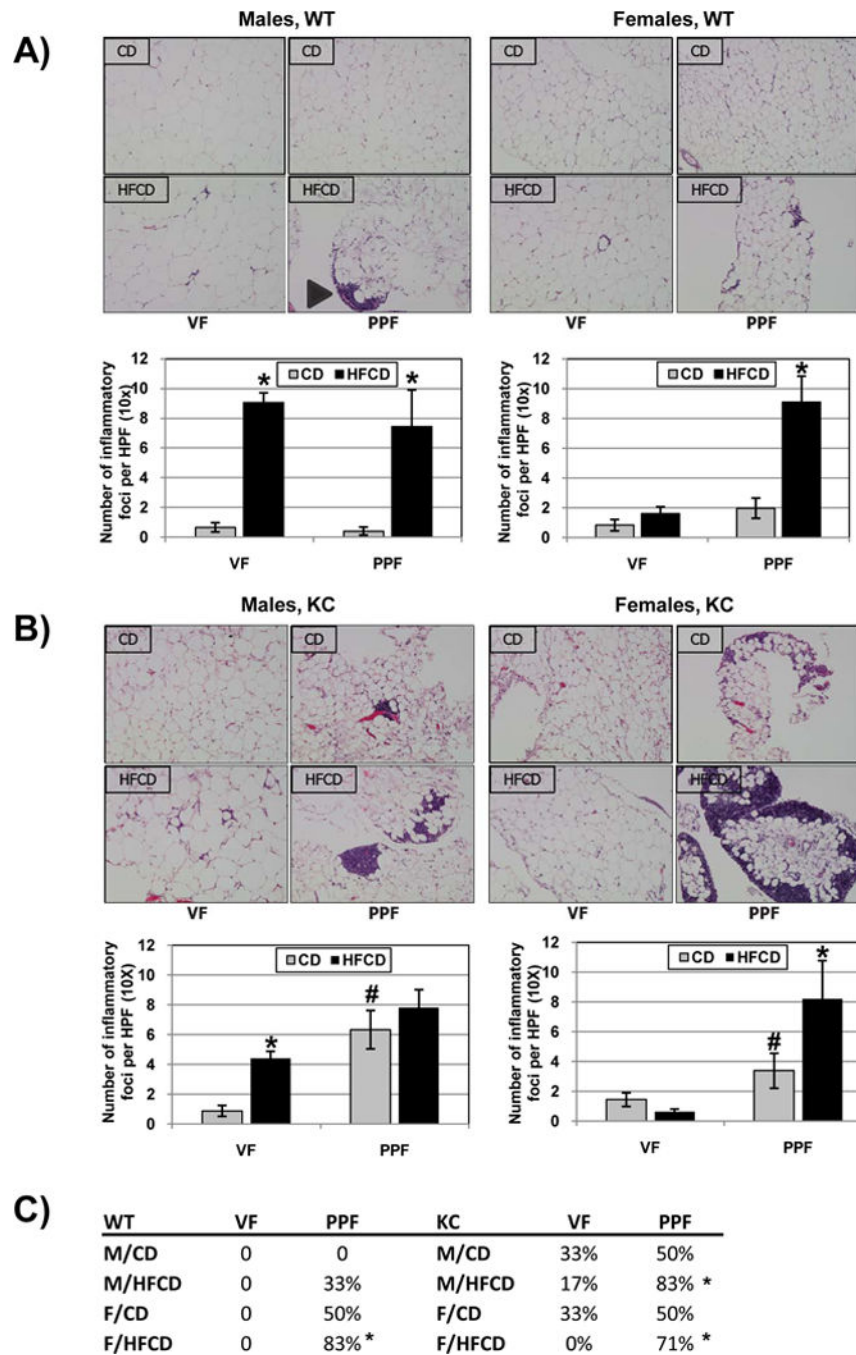


Figure 2. Inflammatory foci in male and female WT (A) and KC (B) mice on the CD and HFCD were quantified. Representative histological images are shown in the upper rows. *, $p < 0.05$, HFCD vs. CD; #, $p < 0.05$, KC vs. WT. (C) The number of animals with larger lymphoid aggregates in either fat depot was counted and shown as a percentage of the total number of animals experimental group. *, $p < 0.05$, PPF vs. VF

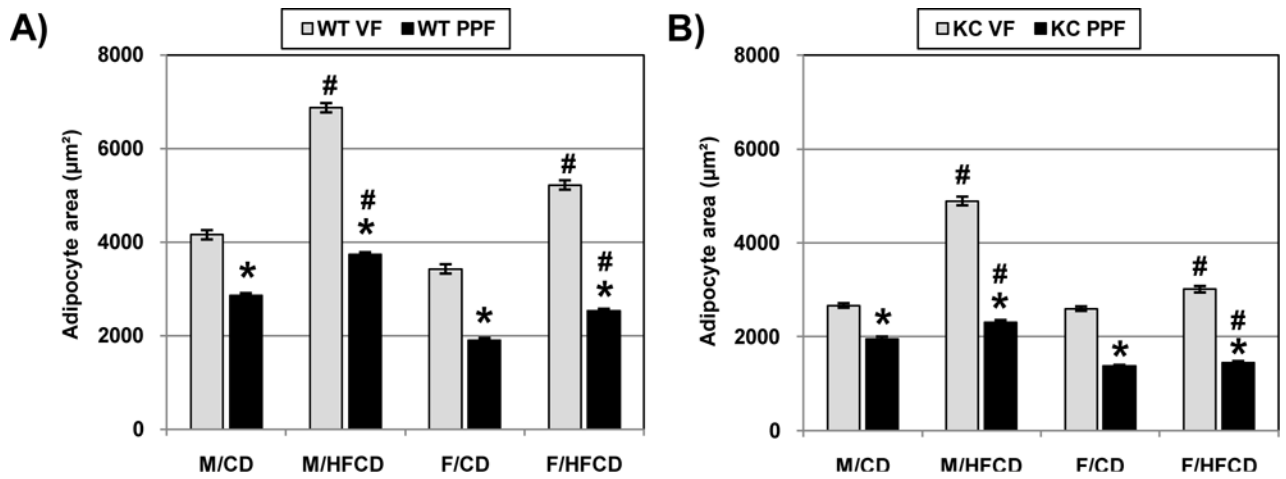


Figure 3.

The size of adipocytes in the visceral (VF) and peri-pancreatic fat (PPF) depot were measured in both WT (A) and KC (B) mice. Ten images were taken per mouse, and 10 adipocytes were measured per image. The area is represented as the mean \pm SEM. *, $p < 0.05$, PPF vs. VF; #, $p < 0.05$, HFCD vs. CD

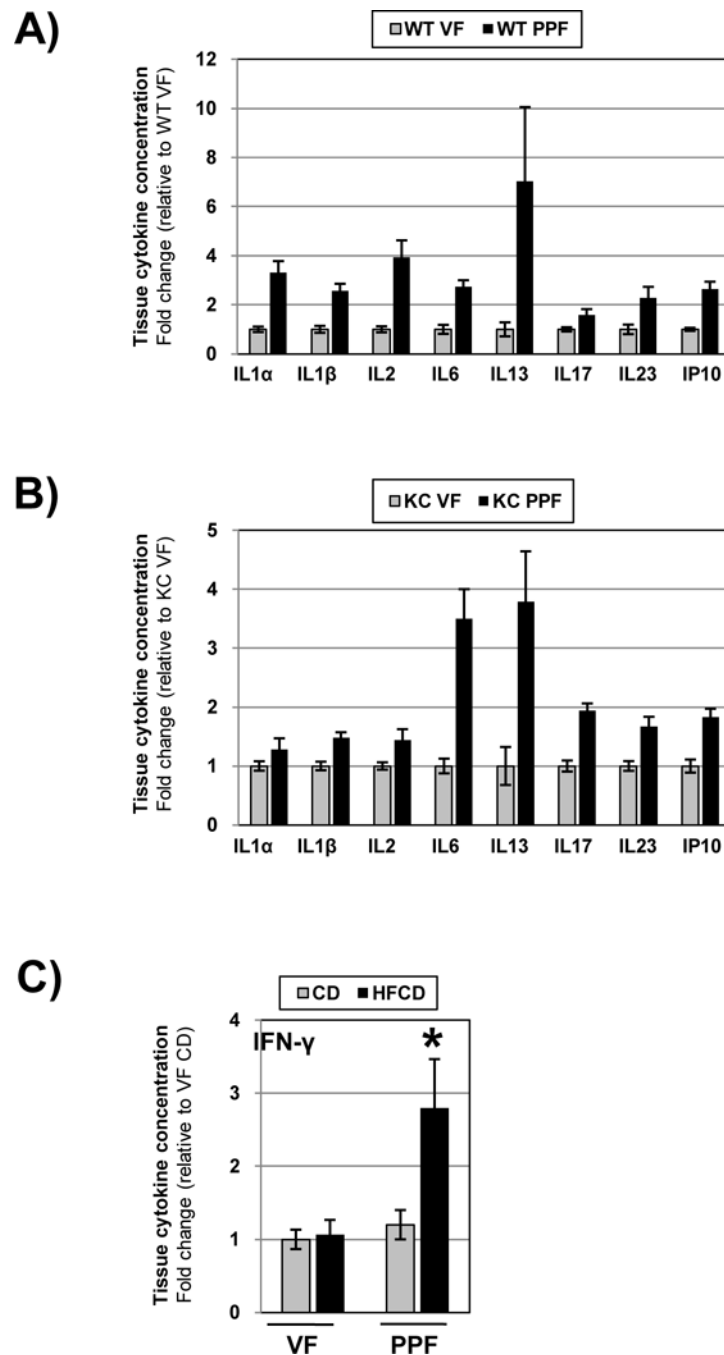


Figure 4.

Tissue cytokine levels in the VF and PPF depots were measured by multiplex. Tissue levels of selected cytokines in the VF were normalized to 1 and fold changes in the PPF depicted in WT (A) and KC (B) mice. Data are presented as mean \pm SEM. Tissue levels of IFN- γ in the VF and PPF of mice fed the CD and HFCD are depicted in C). *, $p < 0.05$, HFCD vs. CD

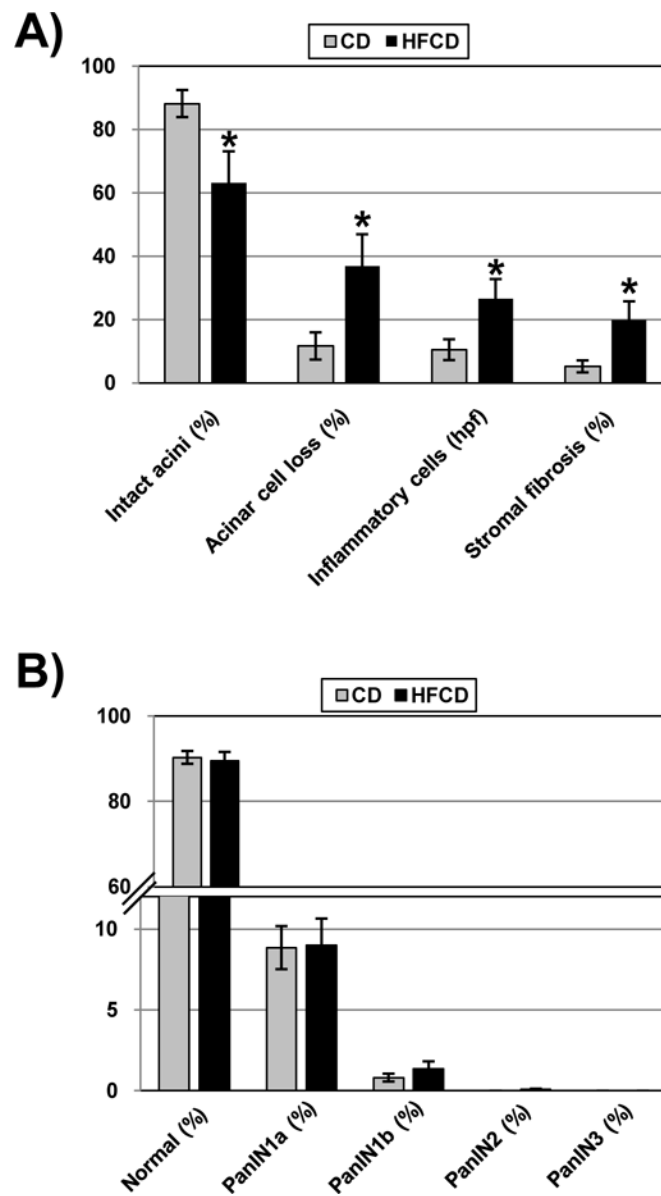


Figure 5. Semiquantitative analyses of inflammatory parameters in the pancreas of mice fed the control diet or HFCD. (A) Percentage (%) of intact acini, percentage (%) of acinar cell loss, number of inflammatory cells per HPF, and percentage (%) of stromal fibrosis were analyzed. *, $p < 0.05$, HFCD vs. CD. (B) Distribution (in %) of normal pancreatic ducts and mPanIN-1a, mPanIN-1b, mPanIN-2, and mPanIN-3 lesions in the pancreas of mutant mice fed the CD or HFCD for 10 weeks.